

# Ni(NHC)]-Catalyzed Cycloaddition of Diynes and Tropone: Apparent Enone Cycloaddition Involving an $8\pi$ Insertion

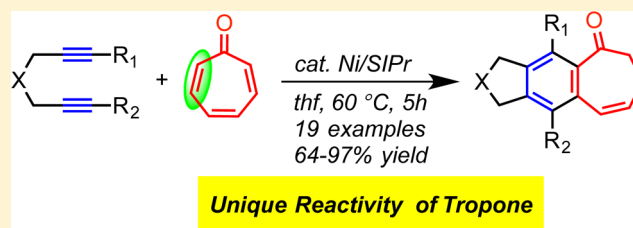
Puneet Kumar,<sup>†,‡,§</sup> Ashish Thakur,<sup>†,§</sup> Xin Hong,<sup>||</sup> K. N. Houk,<sup>\*,||</sup> and Janis Louie<sup>\*,†</sup>

<sup>†</sup>Department of Chemistry, University of Utah, 315 South 1400 East, Salt Lake City, Utah 84112-0850, United States

<sup>||</sup>Department of Chemistry and Biochemistry, University of California, Los Angeles, California 90095, United States

**S** Supporting Information

**ABSTRACT:** A Ni/N-heterocyclic carbene catalyst couples diynes to the C( $\alpha$ )-C( $\beta$ ) double bond of tropone, a type of reaction that is unprecedented for metal-catalyzed cycloadditions with aromatic tropone. Many different diynes were efficiently coupled to afford [5–6–7] fused tricyclic products, while [5–7–6] fused tricyclic compounds were obtained as minor byproducts in a few cases. The reaction has broad substrate scope and tolerates a wide range of functional groups, and excellent regioselectivity is found with unsymmetrical diynes. Theoretical calculations show that the apparent enone cycloaddition occurs through a distinctive  $8\pi$  insertion of tropone. The initial intramolecular oxidative cyclization of diyne produces the nickelacyclopentadiene intermediate. This intermediate undergoes an  $8\pi$  insertion of tropone, and subsequent reductive elimination generates the [5–6–7] fused tricyclic product. This initial product undergoes two competing isomerizations, leading to the observed [5–6–7] and [5–7–6] fused tricyclic products.



Tropone is a readily available seven-membered nonbenzenoid aromatic compound that can undergo cycloadditions to afford complex bridged motifs of a variety of natural products and medicinally important compounds (Figure 1a).<sup>1–4</sup> The

oxygen atom as in (8 + 2)<sup>9</sup> and (8 + 3)<sup>10</sup> cycloaddition reactions (Figure 1a).<sup>11</sup>

Reactions involving tropone as an enone moiety are rare. The exception involves disrupting the conjugation of tropone by precomplexation with iron–carbonyl (eq 1).<sup>12</sup> Although this

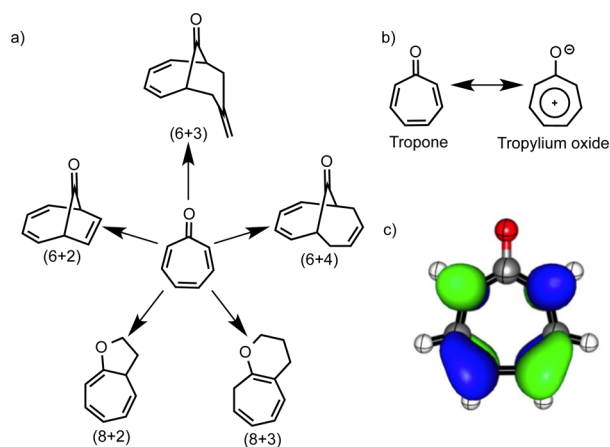
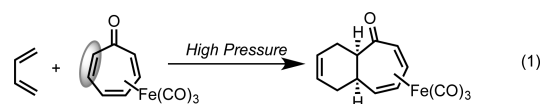


**Figure 1.** (a) Common tropone cycloadditions. (b) Tropone–tropylium oxide resonance. (c) LUMO of tropone computed by HF/6-311+G(d,p).

tropone cycloaddition reactivity can be generally understood by its resonance contributor, tropylium oxide (Figure 1b). This resonance structure explains the dipolar nature of tropone<sup>3a</sup> and the large LUMO coefficients at the alpha-positions (Figure 1c).<sup>5</sup> Therefore, tropone cycloaddition reactions usually lead to bond formations at the  $\alpha$ -positions as in (6 + 2),<sup>6</sup> (6 + 3),<sup>7</sup> and (6 + 4)<sup>8</sup> cycloaddition reactions or in one  $\alpha$ -position and the



approach affords the desired nonbridged bicyclic products, such reactions require stoichiometric amounts of metal complexes as a protecting group for the other two double bonds. This inability to utilize tropones as enones is unfortunate, since selective activation of a single C–C  $\pi$ -bond in cycloaddition would greatly expand the synthetic utility of tropones, given the frequent occurrence of nonbridged seven-membered ring systems in biologically relevant compounds.<sup>4</sup> We describe a solution to the long-standing problem of utilizing tropone as an enone through the use of a highly effective nickel catalyst that couples diynes with a single double bond of a tropone selectively to form fused tricyclic frameworks (vs bridged frameworks) *without the need for precomplexation*.

## RESULTS AND DISCUSSION

Simple enones are known to undergo Ni-catalyzed cycloaddition with diynes (eq 2).<sup>13</sup> However, these conditions fail to provide any cycloadduct product with tropone as shown in

Received: October 13, 2014

Published: November 21, 2014

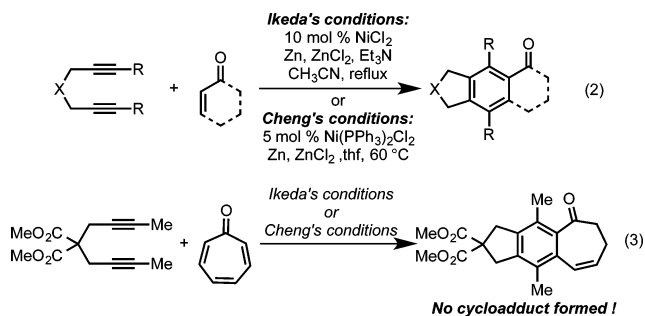


**Table 1. Ni-Catalyzed Cycloaddition of Diyne with Troponone<sup>a</sup>**

1 + a  $\xrightarrow{\text{Cat. Ni/L}_n}$  1a

IMes, I'Bu, IPr, SIPr

entry	L <sub>n</sub>	Ni:L <sub>n</sub>	% conv of 1 <sup>b</sup>	% yield of 1a <sup>b</sup>
1	PPh <sub>3</sub>	1:2	>99	14
2	PCy <sub>3</sub>	1:2	>99	29
3	P(O <sup>i</sup> Pr) <sub>3</sub>	1:2	>99	14
4	PPh <sub>2</sub> Me	1:2	>99	9
5	P( <i>o</i> -tolyl) <sub>3</sub>	1:2	>99	3
6	DPPF	1:1	>99	4
7	BINAP	1:1	85	6
8	DPPB	1:1	>99	6
9	Xantphos	1:1	>99	—
10	<sup>t</sup> Bu-Xantphos	1:1	>99	—
11	IMes	1:2	96	79
12	I'Bu	1:2	98	71
13	IPr	1:2	>99	>99 (92) <sup>c</sup>
14	SIPr	1:2	>99	>99 (92) <sup>c</sup>
15	SIPr	1:2	>99	>99 (95) <sup>c,d</sup>

<sup>a</sup>Reaction conditions: 10 mol % of Ni(cod)<sub>2</sub>, 20 mol % of L, diyne (1 equiv, 0.1 M), troponone (1.1 equiv), toluene, 60 °C, 5 h. <sup>b</sup>Determined by GC using naphthalene as an internal standard. <sup>c</sup>Isolated yield. <sup>d</sup>THF was used instead of toluene.

eq 3. Thus, we focused our investigation on discovering an alternative Ni-catalyzed cycloaddition protocol.

Diyne **1** and troponone **a** were used as model substrates and were subjected to a catalytic amount of Ni(0) and a variety of phosphine and *N*-heterocyclic carbene (NHC) ligands (eq 4). Reactions run with monodentate and bidentate phosphines mostly afforded dimerization of diyne along with traces or low amounts of the desired cycloadduct (Table 1, entry 1–10). However, reactions run with NHCs resulted in good to excellent yields of cycloadduct **1a**, which couples the diyne with a *single C–C double bond* of the troponone selectively (entries 11–15). Ultimately, SIPr proved to be the best ligand. Further optimization led to our final reaction conditions: diyne (1 equiv), troponone (1.1 equiv), 3 mol % of Ni(cod)<sub>2</sub>, 6 mol % of SIPr, THF, 60 °C, and 5 h.

The model substrates afforded the desired product **1a** along with another isomer **1a'** in excellent yield and >90% selectivity for **1a** (eq 5).<sup>14</sup> Similarly, cycloaddition of sulfonamide diyne **2**

**Table 2. Ni-Catalyzed Cycloaddition of Diynes (3–19) and Troponone (a)<sup>a,b</sup>**

3 + a  $\xrightarrow{\text{Cat. Ni/L}_n}$  3a

IMes, I'Bu, IPr, SIPr

 <b>3a</b> , 67% (combined yield) <b>3a:3a' = 94:6<sup>c</sup></b>	 <b>3a'</b> , 67% (combined yield) <b>3a:3a' = 94:6<sup>c</sup></b>	 <b>4a</b> , 97% (combined yield) <b>4a:4a' = 93:7<sup>c</sup></b>	 <b>4a'</b> , 97% (combined yield) <b>4a:4a' = 93:7<sup>c</sup></b>
 <b>5a</b> , 87% (combined yield) <b>5a:5a' = 80:20<sup>c</sup></b>	 <b>5a'</b> , 87% (combined yield) <b>5a:5a' = 80:20<sup>c</sup></b>	 <b>6a</b> , 64%	
 <b>7a</b> , 72% <sup>d</sup>	 <b>8a</b> , 81% <i>Regioselectivity &gt;95:5<sup>c</sup></i>	 <b>9a</b> , 91% <i>Regioselectivity &gt;95:5<sup>c</sup></i>	
 <b>10a</b> , 89% <i>Regioselectivity &gt;95:5<sup>c</sup></i>	 <b>11a</b> , 91% <i>Regioselectivity &gt;95:5<sup>c</sup></i>	 <b>12a</b> , 78% <i>Regioselectivity = 82:18<sup>c</sup></i>	
 <b>13a</b> , 75% <i>Regioselectivity = 93:7<sup>c</sup></i>	 <b>14a</b> , 86% <i>Regioselectivity &gt;95:5<sup>c</sup></i>	 <b>15a</b> , 79% <i>Regioselectivity &gt;95:5<sup>c</sup></i>	
 <b>16a</b> , 65% <i>Regioselectivity &gt;95:5<sup>c</sup></i>	 <b>17a</b> , 70% <i>Regioselectivity &gt;95:5<sup>c</sup></i>		
 <b>18a</b> , 77% (combined yield) <b>18a:18a' = 93:7<sup>c</sup></b> <i>Regioselectivity &gt;95:5<sup>c</sup></i>	 <b>18a'</b> , 77% (combined yield) <b>18a:18a' = 93:7<sup>c</sup></b> <i>Regioselectivity &gt;95:5<sup>c</sup></i>	 <b>19a</b> , 76% <i>Regioselectivity &gt;95:5<sup>c</sup></i>	

<sup>a</sup>Reaction conditions: diyne (1 equiv, 0.1 M), troponone (1.2 equiv), 3 mol % of Ni(cod)<sub>2</sub>, 6 mol % of SIPr, THF, 60 °C, 5 h. <sup>b</sup>Isolated yields (in black), ratio of major and minor cycloadducts (in blue), ratio of major and minor regioisomers (in red). <sup>c</sup>The ratios were determined by <sup>1</sup>H NMR of crude reaction mixture. <sup>d</sup>The reaction was performed with 10 mol % catalyst loading at room temperature.

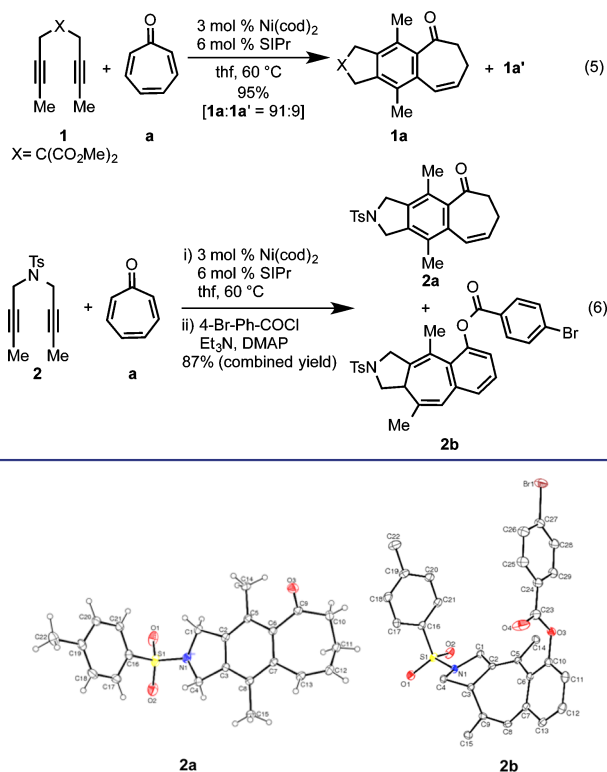


Figure 2. Ortep diagram of **2a** and **2b**.

afforded a mixture of major and minor isomers **2a** and **2a'** respectively, which on subsequent treatment with *p*-bromobenzoyl chloride/ $NEt_3$ /DMAP afforded major isomer **2a** in 74% yield and *p*-bromobenzoyl derivative of minor isomer (**2b**) in 13% yield (eq 6) as crystalline solids (Figure 2). Surprisingly, **2b** (and, therefore, **2a'** as well) has [5–7–6] ring fusion compared to [5–6–7] in the case of the major isomer, **2a**.<sup>15</sup>

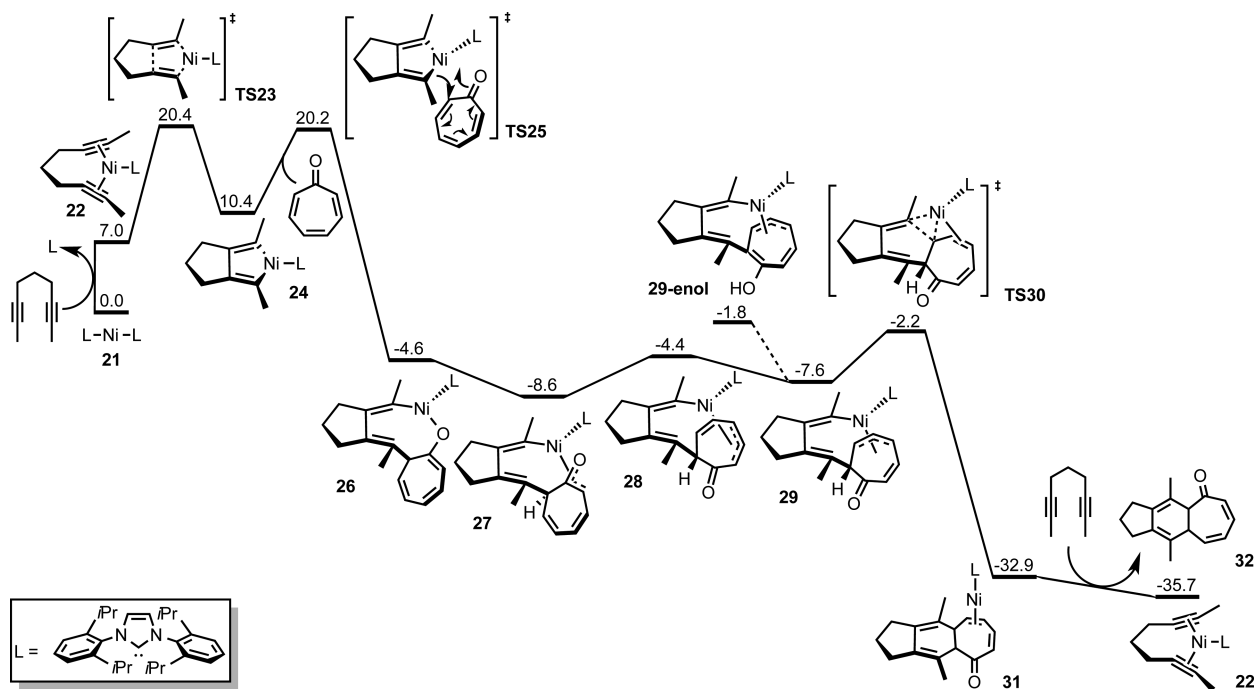


Figure 3. The homocoupling pathway A of  $[Ni(IPr)]$ -catalyzed cycloaddition between nona-2,7-diyne **1** and tropone. Free energies (298 K) with respect to **21** are shown in kcal/mol.

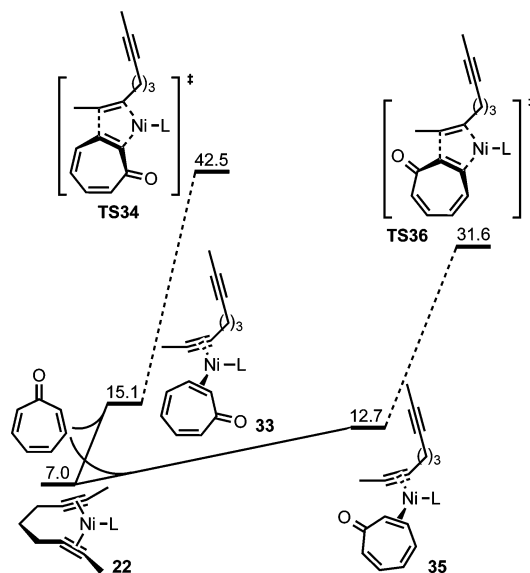
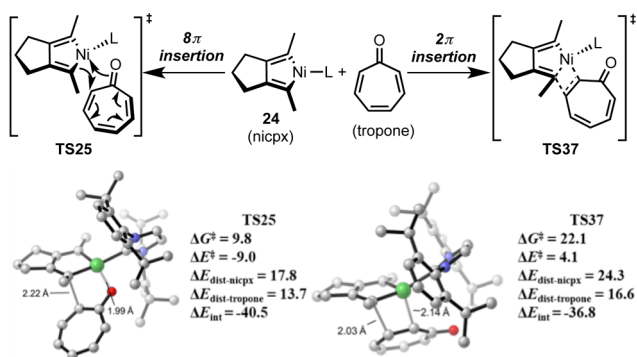


Figure 4. The heterocoupling pathway B of  $[Ni(IPr)]$ -catalyzed cycloaddition between nona-2,7-diyne and tropone. Free energies (298 K) with respect to **21** are shown in kcal/mol.

With optimized reaction conditions in hand, the substrate scope was explored (Table 2). The cycloaddition occurred smoothly with the diyne bearing a sulfone backbone to form **3a** along with minor isomer **3a'**. Notably, this diyne is completely unreactive in several reported Ni-catalyzed cycloadditions.<sup>16</sup> Although Ni catalysts have been reported to catalyze the cycloaddition of nitriles and diynes to form pyridines,<sup>16b,d</sup> diyne **4**, which has a nitrile group in the backbone, selectively reacted with tropone to afford the desired cycloadducts (**4a** and **4a'**) in excellent yield. Inspired by Carreira's work, we performed the cycloaddition reaction with **5**, a diyne with a metabolically



**Figure 5.** Optimized structures, Gibbs free energies, and distortion and interaction energies of transition states of 8 $\pi$  insertion (TS25) and 2 $\pi$  insertion (TS37) of tropone. The Gibbs free energy changes (298 K) with respect to 24 are shown in kcal/mol.

stable backbone,<sup>17</sup> to give cycloadduct 5a in good yield along with minor isomer 5a'. Aryl substituted internal diynes are one of the most challenging substrates in Ni/NHC-catalyzed cycloaddition reactions.<sup>16e,18</sup> Nevertheless, the reaction of aryl substituted symmetrical diynes with tropone afforded 6a and 7a in good yields. Interestingly, no minor cycloadduct (6a' or 7a') was obtained in these cases. To investigate the effect of electronics on the regioselectivity, we subjected unsymmetrical diynes 8 and 9 to standard reaction conditions; remarkably, exclusive formation of one regioisomer was detected (8a and 9a).

The use of different aryl groups (i.e., 3,4-dimethoxyphenyl and naphthyl) on alkyne terminals is also possible (10a and 11a). Due to recent interest in indole bearing novel compounds,<sup>19</sup> diynes 12 and 13 were investigated. Biaryl cycloadducts (12a, 13a) were formed in very good yield and high regioselectivity. Interestingly, the regioselectivity was higher in the case of 3-substituted indole diyne than 5-substituted indole diyne (13a vs 12a). Cycloaddition of phenyl-ethyl diyne 14 and phenyl-silyloxymethyl 15 afforded regioisomers 14a and 15a, where the carbonyl resides next to the phenyl ring, exclusively, while a diyne with covalently bound  $\delta$ -tocopherol can also be easily clicked together with tropone to afford regioselective cycloadduct 16a. An unsymmetrical diyne bearing an internal *gem*-dimethyl group reacted with tropone to afford an exclusive regioisomer 17a, which suggests that regioselectivity is highly dependent on the substituents on the alkyne units of a diyne rather than backbone.<sup>20</sup> The cycloaddition of unsymmetrical isopropyl-methyl diyne (18) afforded products 18a and 18a', where the bulkier group is next to the carbonyl of tropone. Cycloaddition of phenyl-isopropyl diyne 19 affords a product where the isopropyl group is away from the carbonyl group (19a), suggesting that electronic factors override the steric factors (19a). Unfortunately, terminal diynes did not afford any cycloaddition product with tropone due to their high propensity to oligomerize under our reaction conditions.<sup>21,22</sup>

The lack of general methods to access troponoids prompted our investigation on the ability to convert the cycloadduct to a fully aromatized product. We found that compound 2a

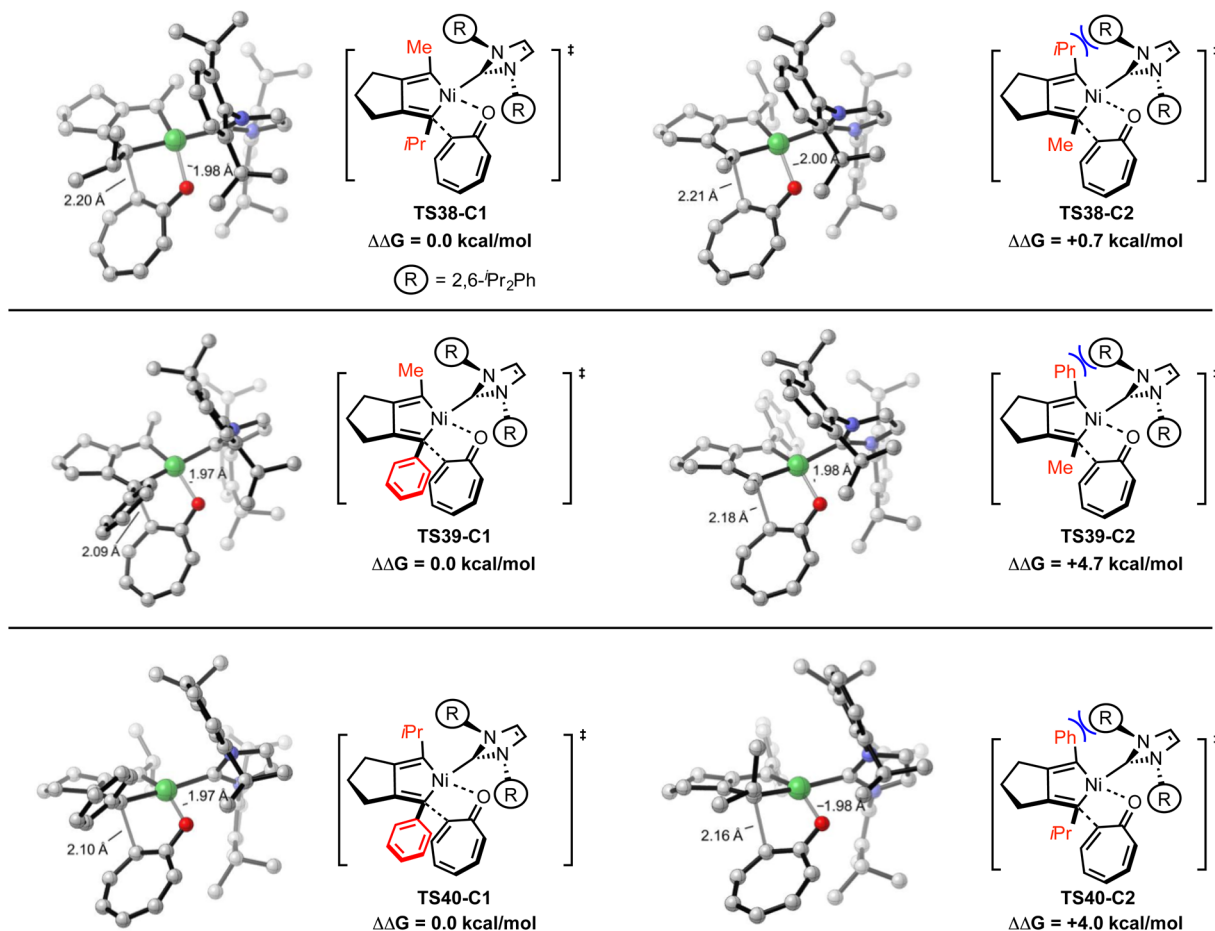


**Figure 6.** Transition states for the intermolecular insertion of tropone into Ni(IPr)-unsymmetrical diyne complexes.

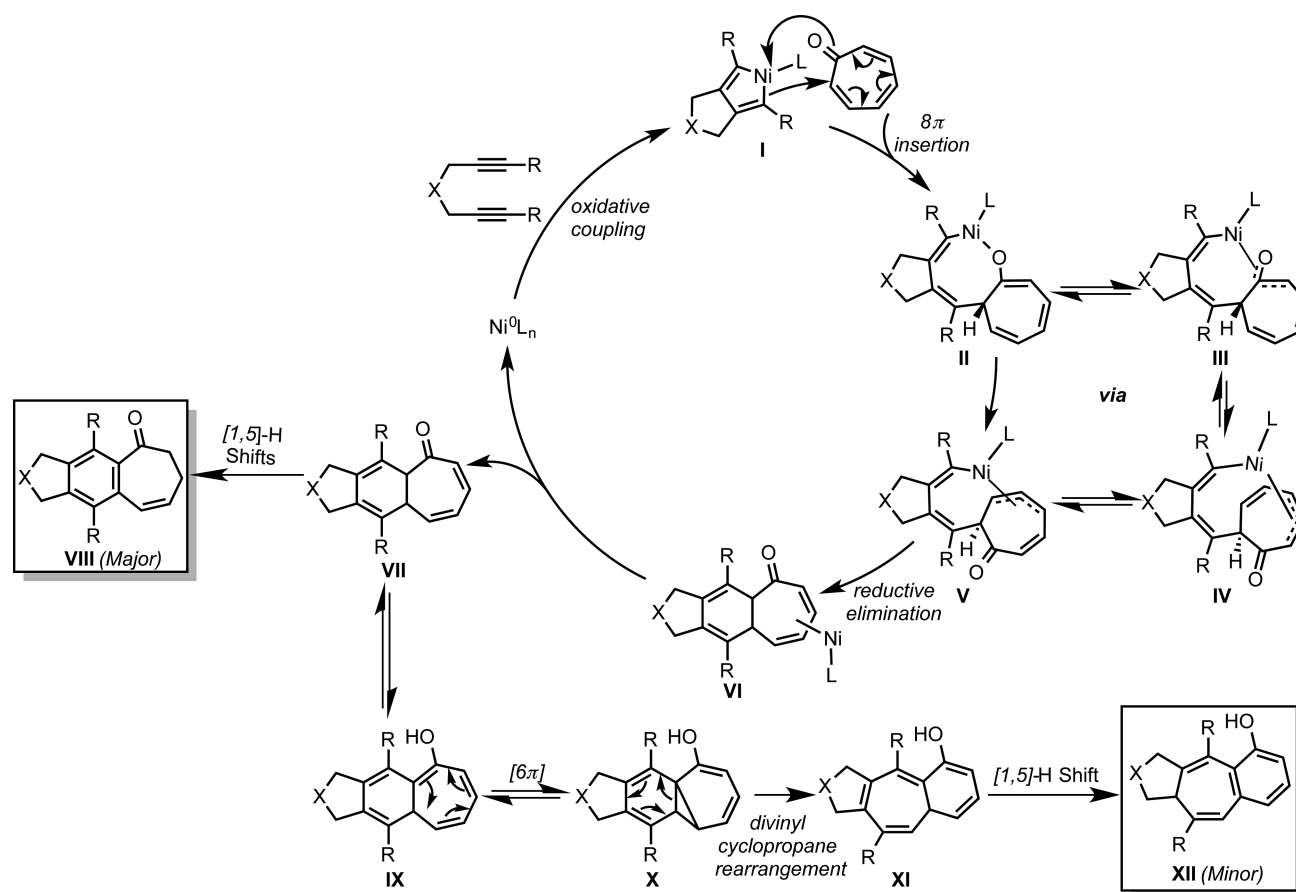
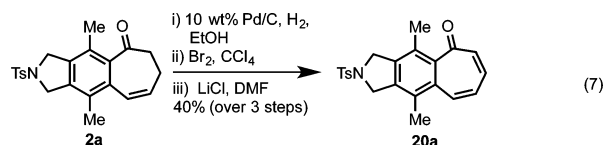


Figure 7. Proposed mechanism for the Ni-catalyzed cycloaddition of diynes and tropone.

can be consistently converted to tropone **20a** by a three-step protocol.<sup>23</sup> The hydrogenation of alkene **2a** led to a saturated cycloheptanone, which was then subjected to dibromination. Finally, dibromination afforded the desired tropone, **20a** (eq 7).



## COMPUTATIONAL MECHANISTIC ANALYSIS

We also undertook a mechanistic investigation of this reaction. Specifically, we studied the catalytic cycles for  $[\text{Ni}(\text{IPr})_2]$ -catalyzed cycloaddition of nona-2,7-diyne and tropone with DFT calculations.<sup>24</sup> Homocoupling,<sup>25</sup> where two alkynes undergo initial oxidative coupling, and heterocoupling,<sup>26</sup> where an alkyne and the tropone undergo initial oxidative coupling, were both investigated.

The free energy changes for the homocoupling pathway are shown in Figure 3. From  $[\text{Ni}(\text{IPr})_2]$  complex **21**, the coordination of diyne to form intermediate **22** is endergonic by 7.0 kcal/mol. Subsequent intramolecular oxidative cyclization via **TS23** requires a 13.4 kcal/mol barrier with respect to **22**, generating the metallacyclopentadiene intermediate **24**. This intermediate undergoes a facile  $8\pi$  insertion (instead of  $2\pi$  insertion, vide infra) of tropone via **TS25**, with a barrier of only 9.8 kcal/mol. The  $8\pi$  insertion produces the eight-membered ring intermediate **26** with the tropone oxygen coordinated to nickel.

The tropone piece of complex **26** can coordinate to nickel in four different fashions, generating the complexes **26** to **29**.<sup>27</sup> The four isomers have similar stabilities, and complex **29** undergoes reductive elimination via **TS30** to give the product-coordinated complex **31**. Product extrusion from **31** is exergonic by 2.8 kcal/mol to release the product and regenerate the nickel-diyne complex **22**. The tautomerization of intermediate complex **29** to **29-enol** is endergonic by 5.8 kcal/mol, and subsequent reductive elimination from **29-enol** will form the 5–7–6 tricyclic product; however, the irreversible reductive elimination via **TS30** suggests that the 5–7–6 tricyclic product arises from Ni-free tautomerization.

The calculations indicate that the resting state of pathway A is  $[\text{Ni}(\text{IPr})_2]$  complex **21**, and oxidative cyclization through **TS23** is the rate-limiting step of the catalytic cycle. The overall reaction barrier is 20.4 kcal/mol, which is consistent with the experimental conditions (60 °C, 5 h). In contrast, the heterocoupling pathway of  $[\text{Ni}(\text{IPr})_2]$ -catalyzed cycloaddition between nona-2,7-diyne and tropone displays higher free energies (Figure 4). Specifically, from nickel-diyne complex **22**, the intermolecular oxidative cyclization between alkyne and tropone can occur via **TS34**, with the carbonyl group of tropone distal to the forming C–C bond. This step requires a barrier of 42.5 kcal/mol with respect to the  $[\text{Ni}(\text{IPr})_2]$  complex **21**, which is much less favorable as compared to the homocoupling pathway discussed above (Figure 4). Alternatively, the intermolecular cyclization can occur with the tropone carbonyl group proximal to the forming C–C bond, as in **TS36**. **TS36** is 31.6 kcal/mol higher in free energy than the resting state **21**, which is also less favorable than the productive homocoupling pathway. Therefore, unlike other

Ni-catalyzed couplings between alkynes and carbonyls,<sup>16e,28</sup> a heterocoupling mechanism is not operative in the [Ni(IPr)]-catalyzed cycloaddition between diyne and tropone.

Next, insertion of the tropone was investigated, and two probable pathways emerged: a traditional  $2\pi$  insertion and a distinctive  $8\pi$  insertion. The transition states of  $8\pi$  (TS25) and  $2\pi$  insertion (TS37) of tropone were both located, and their free energies and structures are shown in Figure 5.<sup>29</sup> Interestingly, the  $8\pi$  insertion is found to be more favorable by 12.3 kcal/mol.

We studied the origins of this preference by employing the distortion/interaction model on TS25 and TS37.<sup>30</sup> The distortion energy reflects the structural changes from nickel complex **24** or tropone to the corresponding geometries in the transition states, and the interaction energy is the energy of interactions between the distorted fragments, computed as the difference between the activation energy and the total distortion energy. The difference between the distortion energies of TS25 and TS37 is the major reason for the preference for  $8\pi$  insertion. The distortion energy is 17.8 kcal/mol energy for **24** and 13.7 kcal/mol energy for tropone to achieve the distorted geometries in TS25, while it requires much larger distortions (24.3 kcal/mol for **24** and 16.6 kcal/mol for tropone) in TS37. Stronger steric repulsions are generated between the nickelacyclopentadiene moiety and tropone in TS37 as compared to those in TS25. This difference between the steric repulsions eventually leads to the preference of the unconventional  $8\pi$  insertion, and this is the highest order of poly- $\pi$  insertion so far.<sup>31</sup>

**Regioselectivity.** The transition states for the  $8\pi$  insertion of tropone with unsymmetrical diynes were also studied. For the isopropyl–methyl diyne (Figure 6), the transition state TS38-C1 that contains the bulky isopropyl group on the diyne next to tropone is more stable than TS38-C2 by 0.7 kcal/mol to avoid steric repulsions between the isopropyl group and IPr ligand. For phenyl–methyl diyne, the transition state TS39-C1 is 4.7 kcal/mol more stable than TS39-C2 mainly due to the steric repulsions between the phenyl group and the bulky NHC ligand in TS39-C1. Also, for phenyl–isopropyl diyne, the phenyl group is more sterically demanding, and a 4.0 kcal/mol preference to the TS40-C1 is found.

Overall, our data suggest that Ni-catalyzed cycloaddition occurs via the mechanism shown in Figure 7. The homo-oxidative coupling of diyne on Ni(0) forms Ni(II)–cyclopentadiene intermediate **I** that undergoes  $8\pi$  insertion of tropone to afford seven-membered ring complex **II**. Intermediate **II** isomerizes from oxygen coordination to  $\eta^3$ -coordination resulting in intermediate **III**, which can subsequently isomerize to an  $\eta^3$ -coordinated-Ni(II) complex **V** through intermediates **IV**. Finally intermediate **V** reductively eliminates to give **VI**, which releases the tricyclic product, **VII**, and regenerates the Ni(0) catalyst. At this point, compound **VII** can preferentially aromatize via sigmatropic shifts to afford major product **VIII**. However, a minor pathway involves tautomerization of **VII** to cycloheptatrienol **IX**, which undergoes further  $6\pi$  electrocyclicization to afford an interesting bis(divinyl)–cyclopropane intermediate, **X**. Intermediate **X** can either revert to **IX** or irreversibly rearrange to [5–7–6] fused intermediate **XI**, which undergoes further sigmatropic shifts to yield the observed minor product, **XII**. This sigmatropic shift could be catalyzed by a trace amount of water through the bridge of one or multiple molecules of water.<sup>32</sup> Due to the uncertainty of the catalyst, we did not perform computational studies on the isomerization of the tricyclic product **VII**.

In conclusion, we have discovered a nickel catalyst that can effectively and selectively incorporate a single C–C  $\pi$ -bond of

tropone in the cycloaddition with diynes. We have also successfully converted these cycloadducts to useful troponoids. The mechanism of this novel cycloaddition reaction has been investigated using DFT calculations. It involves a unique  $8\pi$  insertion of tropone to form the observed major and minor products. The mechanistic studies to further understand this unique reactivity of tropone and application of this chemistry are underway in our laboratories.

## ■ ASSOCIATED CONTENT

### 📄 Supporting Information

General experimental information, synthesis of diynes, spectroscopic characterizations, crystallographic analyses (CIF), and computational data. This material is available free of charge via the Internet at <http://pubs.acs.org>.

## ■ AUTHOR INFORMATION

### Corresponding Authors

louie@chem.utah.edu

houk@chem.ucla.edu

### Present Address

‡P.K.: Discovery Chemistry, Merck & Co. Inc., Rahway, New Jersey, United States.

### Author Contributions

§P.K. and A.T. contributed equally.

### Notes

The authors declare no competing financial interest.

## ■ ACKNOWLEDGMENTS

J.L. thanks the NIH (GM076125) and NSF (CHE-0911017) for financial support of this work. K.N.H. thanks the NSF (CHE-1361104) for financial support of this research. We thank Drs. J. Muller and A. Arif for providing HRMS and X-ray spectroscopic data, respectively. Calculations were performed on the Hoffman2 Cluster at UCLA and the Extreme Science and Engineering Discovery Environment (XSEDE), which is supported by the NSF (OCI-1053575).

## ■ REFERENCES

- (1) Clayden, J.; Greeves, N.; Warren, S.; Wothers, P. In *Organic Chemistry*; Oxford University Press Inc.: New York, 2012.
- (2) (a) Dewar, M. J. S. *Nature* **1945**, *155*, 50. (b) Dewar, M. J. S. *Nature* **1945**, *155*, 141. (c) Dauben, H. J., Jr.; Reingold, H. J. *J. Am. Chem. Soc.* **1951**, *73*, 876. (d) Doering, W. v. E.; Detert, F. L. *J. Am. Chem. Soc.* **1951**, *73*, 877. (e) Katsura, S.; Sato, K.; Akaishi, K.; Nozoe, T.; Seto, S.; Kitahara, Y. *Proc. Jpn. Acad.* **1951**, *27*, 36. (f) Tamelen, E. E. v.; Hildahl, G. T. *J. Am. Chem. Soc.* **1953**, *75*, 5451.
- (3) (a) Pauson, P. L. *Chem. Rev.* **1955**, *55*, 9. (b) Kurita, Y.; Seto, S.; Nozoe, T.; Kubo, M. *Bull. Chem. Soc. Jpn.* **1953**, *26*, 272.
- (4) Bentley, R. *Nat. Prod. Rep.* **2008**, *25*, 118.
- (5) Fleming, I. In *Frontier Orbitals and Organic Chemical Reactions*; John Wiley & Sons Ltd.: 1976.
- (6) For (6 + 2) cycloaddition, see: (a) Feldman, K. S.; Come, J. H.; Freyer, A. J.; Kosmider, B. J.; Smith, C. M. *J. Am. Chem. Soc.* **1986**, *108*, 1327. (b) Feldman, K. S.; Come, J. H.; Kosmider, B. J.; Smith, P. M.; Rotell, D. P.; Wu, M.-J. *J. Org. Chem.* **1989**, *54*, 92. (c) Feldman, K. S.; Wu, M.-J.; Rotella, D. P. *J. Am. Chem. Soc.* **1989**, *111*, 6457. (d) Feldman, K. S.; Wu, M.-J.; Rotella, D. P. *J. Am. Chem. Soc.* **1990**, *112*, 8490.
- (7) For (6 + 3) cycloadditions, see: (a) Trost, B. M.; Seoane, P. R. *J. Am. Chem. Soc.* **1987**, *109*, 615. (b) Trost, B. M.; McDougall, P. J.; Hartmann, O.; Wathen, P. T. *J. Am. Chem. Soc.* **2008**, *30*, 14960. (c) Du, Y.; Feng, J.; Lu, X. *Org. Lett.* **2005**, *7*, 1987. (d) Trost, B. M.; McDougall, P. J. *Org. Lett.* **2009**, *11*, 3782. (e) Liu, H.; Wu, Y.; Zhao,

Y.; Li, Z.; Zhang, L.; Yang, W.; Jiang, H.; Jing, C.; Yu, H.; Wang, B.; Xiao, Y.; Guo, H. *J. Am. Chem. Soc.* **2014**, *136*, 2625. (f) Teng, H.-L.; Yao, L.; Wang, C.-J. *J. Am. Chem. Soc.* **2014**, *136*, 4075.

(8) For a review on (6 + 4) cycloaddition, see: (a) Rigby, J. H. *Org. React.* **1997**, *49*, 331. (b) Ito, S.; Fujise, Y.; Okuda, T.; Inoue, Y. *Bull. Chem. Soc. Jpn.* **1966**, *39*, 1351. (c) Houk, K. N.; Woodward, R. B. *J. Am. Chem. Soc.* **1970**, *92*, 4145. (d) Ito, S.; Sakan, K.; Fujise, Y. *Tetrahedron Lett.* **1970**, *11*, 2873. (e) Mukai, T.; Akasaki, Y.; Hagiwara, T. *J. Am. Chem. Soc.* **1972**, *94*, 675. (f) Ito, S.; Ohtani, H.; Narita, S.; Honma, H. *Tetrahedron Lett.* **1972**, 2223. (g) Sasaki, T.; Kanematsu, K.; Iizuka, K. *J. Org. Chem.* **1976**, *41*, 1105. (h) Mukherjee, D.; Watts, C. R.; Houk, K. N. *J. Org. Chem.* **1978**, *43*, 817. (i) Garst, M. E.; Roberts, V. A.; Prussin, C. *Tetrahedron* **1983**, *39*, 581. (j) Garst, M. E.; Roberts, V. A.; Houk, K. N.; Rondan, N. G. *J. Am. Chem. Soc.* **1984**, *106*, 3882. (k) Paquette, L. A.; Hathaway, S. J.; Schrich, P. F. *T. J. Org. Chem.* **1985**, *50*, 4199. (l) Rigby, J. H.; Moore, T. L.; Rege, S. *J. Org. Chem.* **1986**, *51*, 2398. (m) Funk, R. L.; Bolton, G. L. *J. Am. Chem. Soc.* **1986**, *108*, 4655. (n) Rigby, J. H.; Cuisiat, S. V. *J. Org. Chem.* **1993**, *58*, 6286. (o) Rigby, J. H.; Rege, S. D.; Sandanayaka, V. P.; Kirova, M. *J. Org. Chem.* **1996**, *61*, 842. (p) Lubineau, A.; Bouchain, G.; Queneau, Y. *J. Chem. Soc., Perkin Trans. 1* **1997**, 2863. (q) Isakovic, L.; Ashenurst, J. A.; Gleason, J. L. *Org. Lett.* **2001**, *3*, 4189. (r) Rigby, J. H.; Bazin, B.; Meyer, J. H.; Mohammadi, F. *Org. Lett.* **2002**, *4*, 799. (s) Rigby, J. H.; Chouraqui, G. *Synlett* **2005**, 2501. (t) Pidaparthi, R. R.; Welker, M. E.; Day, C. S. *Organometallics* **2006**, *25*, 974. (u) Ashenurst, J. A.; Gleason, J. L. *Tetrahedron Lett.* **2008**, *49*, 504. (v) Isakovic, L.; Ashenurst, J. A.; Gleason, J. L. *Tetrahedron Lett.* **2010**, *66*, 368.

(9) For a review on (8 + 2) cycloaddition, see: (a) Nair, V.; Abhilash, K. G. *Synlett* **2008**, 301. (b) Gompper, R.; Elser, S. W. *Tetrahedron Lett.* **1968**, 1019. (c) Gompper, R. *Angew. Chem., Int. Ed.* **1969**, *8*, 312. (d) Cantrell, T. S. *J. Am. Chem. Soc.* **1971**, *93*, 2540. (e) Li, Z.-H.; Hirayama, S.; Kato, N.; Mori, A.; Takeshita, H. *Rep. Inst. Adv. Mater. Study* **1991**, *6*, 331. (f) Kumar, K.; Kapur, A.; Ishar, M. P. S. *Org. Lett.* **2000**, *2*, 787. (g) Okamoto, J.; Yamabe, S.; Minato, T.; Hasegawa, T.; Machiguchi, T. *Helv. Chim. Acta* **2005**, *88*, 1519. (h) Li, P.; Yamamoto, H. *J. Am. Chem. Soc.* **2009**, *131*, 16628.

(10) For (8 + 3) cycloaddition, see: (a) Ishizu, T.; Mori, M.; Kanematsu, K. *J. Org. Chem.* **1981**, *46*, 526. (b) Nair, V.; Poonoth, M.; Vellath, S.; Suresh, E.; Thirumalai, R. *J. Org. Chem.* **2006**, *71*, 8964. (c) Thangaraj, M.; Bhojgude, S. R.; Bisht, R. H.; Gonnade, R. G.; Biju, A. T. *J. Org. Chem.* **2014**, *79*, 4757.

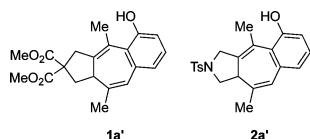
(11) Besides these higher order cycloadditions, tropone also participates in (4 + 2) cycloaddition reactions. For examples, see: ref 8m, ref 9h, and (a) Rigby, J. H.; Sage, J.-M.; Raggon, J. *J. Org. Chem.* **1982**, *47*, 4815. (b) Ishar, M. P. S.; Gandhi, P. R. *Tetrahedron* **1993**, *49*, 6729. (c) Asao, T.; Ito, S.; Murata, I. *Eur. J. Org. Chem.* **2004**, 899. (d) Li, P.; Yamamoto, H. *Chem. Commun.* **2010**, *46*, 6294.

(12) (a) Franck-Neumann, M.; Martina, D. *Tetrahedron Lett.* **1977**, 2293. (b) Rigby, J. H.; Ogbu, C. O. *Tetrahedron Lett.* **1990**, *31*, 3385.

(13) (a) Ikeda, S.; Watanabe, H.; Sato, Y. *J. Org. Chem.* **1998**, *63*, 7026. (b) Sambaiah, T.; Li, L.-P.; Huang, D.-J.; Lin, C.-H.; Rayabarapu, D. K.; Cheng, C.-H. *J. Org. Chem.* **1999**, *64*, 3663.

(14) Careful spectroscopic analysis of **1a'** (i.e., a broad peak in <sup>1</sup>H NMR and IR as well as the lack of a carbonyl carbon in <sup>13</sup>C NMR) indicated the presence of an -OH functional group. Deuterium exchange reactions also confirmed this functionality.

(15) This analysis reveals the identity of **1a'** and **2a'** as



(16) (a) Duong, H. A.; Cross, M. J.; Louie, J. *J. Am. Chem. Soc.* **2004**, *126*, 11438. (b) McCormick, M. M.; Duong, H. A.; Zuo, G.; Louie, J. *J. Am. Chem. Soc.* **2005**, *127*, 5030. (c) Kumar, P.; Troast, D. M.; Cella, R.; Louie, J. *J. Am. Chem. Soc.* **2011**, *133*, 7719. (d) Kumar, P.;

Prescher, S.; Louie, J. *Angew. Chem., Int. Ed.* **2011**, *50*, 10694. (e) Kumar, P.; Louie, J. In *Transition-metal-mediated aromatic ring construction*; Wiley, Inc.: 2013; Chapter 2.

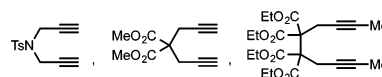
(17) (a) Burkhard, J. A.; Wuitschik, G.; Roger-Evans, M.; Carreira, E. M. *Angew. Chem., Int. Ed.* **2010**, *49*, 9052. (b) Kumar, P.; Zhang, K.; Louie, J. *Angew. Chem., Int. Ed.* **2012**, *51*, 8602. (c) Kumar, P.; Louie, J. *Org. Lett.* **2012**, *14*, 2026. (d) Thakur, A.; Facer, M. E.; Louie, J. *Angew. Chem., Int. Ed.* **2013**, *52*, 12161.

(18) (a) Louie, J.; Gibby, J. E.; Farnworth, M. V.; Tekavec, T. N. *J. Am. Chem. Soc.* **2002**, *124*, 15188. (b) Tekavec, T. N.; Louie, J. *Org. Lett.* **2005**, *7*, 4037. (c) Tekavec, T. N.; Louie, J. *J. Org. Chem.* **2008**, *73*, 2641.

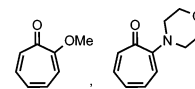
(19) (a) Atta-ur-Rahman; Basha, A. *Indole Alkaloids*; Harwood Academic: Chichester, U.K., 1998. (b) Somai, M.; Yamada, F. *Nat. Prod. Rep.* **2005**, *22*, 73. (c) Thakur, A.; Zhang, K.; Louie, J. *Chem. Commun.* **2012**, *48*, 203.

(20) Tekavec, T. N.; Arif, A. M.; Louie, J. *Tetrahedron* **2004**, *60*, 7431.

(21) Terminal diynes and 2.8-diyne (shown below) failed to provide any cycloaddition product with tropone.



(22) 2-Substituted tropones (shown below) were also unreactive in our cycloaddition with diynes.



(23) Ewing, G. D.; Paquette, L. A. *J. Org. Chem.* **1975**, *40*, 2965.

(24) The optimization was carried out with the B3LYP method, and the SDD basis set for nickel and the 6-31G(d) basis set for the other atoms. The single-point energies and solvent effects in THF were computed with the M06 method, and the SDD basis set for nickel and the 6-311+G(2d,p) basis set for the other atoms. Solvation energies were evaluated using the CPCM model. Computational details are included in the Supporting Information.

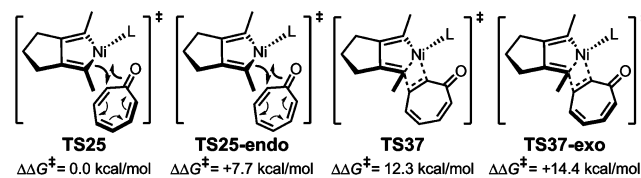
(25) For related computational studies on [Ni(NHC)]-catalyzed homocoupling pathways with diynes, see: (a) Tao, J.-Y.; Fang, D.-C.; Chass, G. A. *Phys. Chem. Chem. Phys.* **2012**, *14*, 6937. (b) Hong, X.; Liu, P.; Houk, K. N. *J. Am. Chem. Soc.* **2013**, *135*, 1456. For a related computational study on tropone, see: (c) Ariafard, A.; Lin, Z. *J. Organomet. Chem.* **2006**, *691*, 4545.

(26) Zhao, Y.; Liu, Y.; Bi, S.; Liu, Y. *J. Organomet. Chem.* **2014**, 758, 45.

(27) The transition states between **26** to **29** could not be located due to the flat potential energy surface. For a related study on the low barrier of coordination change of metal complexes, see: (a) Wei, C. S.; Jiménez-Hoyos, C. A.; Videa, M. F.; Hartwig, J. F.; Hall, M. B. *J. Am. Chem. Soc.* **2010**, *132*, 3078. For a related computational study on the low rotational barrier of  $\pi$  coordination in nickel complexes, see: (b) Sontag, S. K.; Bilbrey, J. A.; Huddleston, N. E.; Sheppard, G. R.; Allen, W. D.; Locklin, J. *J. Org. Chem.* **2014**, *79*, 1836.

(28) Montgomery, J.; Sormunen, G. *Top. Curr. Chem.* **2007**, *279*, 1.

(29) Both *endo* and *exo* transition states are located, and the most favorable ones are shown in Figure 5.



$\Delta\Delta G^\ddagger = 0.0$  kcal/mol  $\Delta\Delta G^\ddagger = +7.7$  kcal/mol  $\Delta\Delta G^\ddagger = 12.3$  kcal/mol  $\Delta\Delta G^\ddagger = +14.4$  kcal/mol

(30) For related studies on the distortion/interaction model in organometallic reactions, see: (a) Garcia, Y.; Schoenebeck, F.; Legault, C. Y.; Merlic, C. A.; Houk, K. N. *J. Am. Chem. Soc.* **2007**, *129*, 12664.

- (b) Legault, C. Y.; Garcia, Y.; Merlic, C. A.; Houk, K. N. *J. Am. Chem. Soc.* **2009**, *131*, 6632. (c) van Zeist, W.-J.; Bickelhaupt, F. M. *Dalton Trans.* **2011**, *40*, 3028. (d) Poater, J.; Feixas, F.; Bickelhaupt, F. M.; Solà, M. *Phys. Chem. Chem. Phys.* **2011**, *13*, 20673. (e) Hong, X.; Liang, Y.; Houk, K. N. *J. Am. Chem. Soc.* **2014**, *136*, 2017. For reviews, see: (f) van Zeist, W.-J.; Bickelhaupt, F. M. *Org. Biomol. Chem.* **2010**, *8*, 3118. (g) Fernández, I. *Phys. Chem. Chem. Phys.* **2014**, *16*, 7662. (h) Fernández, I.; Bickelhaupt, F. M. *Chem. Soc. Rev.* **2014**, *43*, 4953.
- (31) (a) Lobach, M. I.; Kormer, V. A. *Russ. Chem. Rev.* **1979**, *48*, 758. (b) Brookhart, M.; Pinhas, A. R.; Lukacs, A. *Organometallics* **1982**, *1*, 1730.
- (32) (a) Liang, Y.; Liu, S.; Xia, Y.; Li, Y.; Yu, Z.-X. *Chem.—Eur. J.* **2008**, *14*, 4361. (b) Liang, Y.; Zhou, H.; Yu, Z.-X. *J. Am. Chem. Soc.* **2009**, *131*, 17783.